

Aerodynamic Thrust Modelling in Wave Tank Tests of Offshore Floating Wind Turbines Using a Ducted Fan

This content has been downloaded from IOPscience. Please scroll down to see the full text.

2014 J. Phys.: Conf. Ser. 524 012089

(<http://iopscience.iop.org/1742-6596/524/1/012089>)

View [the table of contents for this issue](#), or go to the [journal homepage](#) for more

Download details:

IP Address: 128.39.227.84

This content was downloaded on 16/06/2015 at 10:37

Please note that [terms and conditions apply](#).

Aerodynamic Thrust Modelling in Wave Tank Tests of Offshore Floating Wind Turbines Using a Ducted Fan

José Azcona¹, Faisal Bouchotrouch¹, Marta González¹, Joseba Garcíandía¹, Xabier Munduate¹, Felix Kelberlau², Tor A Nygaard²

¹National Renewable Energy Centre, CENER
Ciudad de la Innovación 7, 31621 Sarriguren, Navarra, Spain
Telephone: +34 948 252 800

²Institute for Energy Technology, IFE
Instituttveien 18, P.O. Box 40, NO-2007 Kjeller, Norway
Telephone: +47 63 816 356

E-mail: jazcona@cener.com

Abstract. Wave tank testing of scaled models is standard practice during the development of floating wind turbine platforms for the validation of the dynamics of conceptual designs. Reliable recreation of the dynamics of a full scale floating wind turbine by a scaled model in a basin requires the precise scaling of the masses and inertias and also the relevant forces and its frequencies acting on the system. The scaling of floating wind turbines based on the Froude number is customary for basin experiments. This method preserves the hydrodynamic similitude, but the resulting Reynolds number is much lower than in full scale. The aerodynamic loads on the rotor are therefore out of scale. Several approaches have been taken to deal with this issue, like using a tuned drag disk or redesigning the scaled rotor.

This paper describes the implementation of an alternative method based on the use of a ducted fan located at the model tower top in the place of the rotor. The fan can introduce a variable force that represents the total wind thrust by the rotor. A system controls this force by varying the rpm, and a computer simulation of the full scale rotor provides the desired thrust to be introduced by the fan. This simulation considers the wind turbine control, gusts, turbulent wind, etc. The simulation is performed in synchronicity with the test and it is fed in real time by the displacements and velocities of the platform captured by the acquisition system. Thus, the simulation considers the displacements of the rotor within the wind field and the calculated thrust models the effect of the aerodynamic damping. The system is not able currently to match the effect of gyroscopic momentum.

The method has been applied during a test campaign of a semisubmersible platform with full catenary mooring lines for a 6MW wind turbine in scale 1/40 at École Centrale de Nantes. Several tests including pitch free decay under constant wind and combined wave and wind cases have been performed. Data from the experiments are compared with aero-servo-hydro-elastic computations with good agreement showing the validity of the method for the representation of the scaled aerodynamics. The new method for the aerodynamic thrust scaling in basin tests is very promising considering its performance, versatility and lower cost in comparison with other methods.



1. Introduction

The installation of offshore wind turbines has several advantages in comparison with onshore locations. The energy yield of a wind turbine installed in open sea is, in general, higher than onshore due to higher and steadier winds. The visual and audible impact of an offshore wind farm is not such an important design restriction as in onshore wind turbines. Finally, most of the world's population is located close to the coastline and transmission losses are low.

When no shallow waters are found close to the coast, as in some parts of the South of Europe, floating platforms have to be used, because bottom fixed substructures are not economically feasible. In the development of floating wind turbine concepts, scaled model tests of combined wave and wind loads are often performed. This is an efficient time and cost saving method of evaluating the dynamics of the design with reliability and low risk. In order to achieve accurate information of the experiments, the dynamic loading coming from wave and wind has to be correctly scaled.

2. Scaling of Wind Thrust in Combined Wave and Wind Tests

Froude scaling has become a standard in the different scaled floating wind turbine test campaigns performed up to date [1]. This methodology has been extensively used in the oil & gas industry, and experience has showed that it is an efficient way of preserving the hydrodynamic similarity. A description of this scaling method can be found in [2]. The realistic inclusion of wind for the testing of a floating wind turbine in combination with waves is a technical challenge, because Froude scaling produce low Reynolds numbers. As the lift and drag coefficients of the blade airfoils are very sensitive to the Reynolds number, the aerodynamic forces on the turbine rotor are out of scale when Froude scaling is directly applied.

One method to deal with this issue consists on the use of a drag disk instead of the rotor. If the dimensions and the drag of the disk are correctly chosen, the wind flow will produce a representative force of the full scale wind loading. With this system the influence of the control logic over the aerodynamic loading cannot be captured and the aerodynamic torque is not accurately modelled. The gyroscopic effects can be taken into account by installing a motor that rotates a mass representing the rotor inertia at the adequate speed. This methodology was used in the WindFloat project [3]. A different approach was taken in the DeepCwind test campaign [4]. The wind turbine model was scaled according to the Froude number. To achieve appropriately scaled thrust forces, the wind speeds had to be increased, but the matching of the aerodynamic characteristics was not good enough. Finally, a more precise alternative consists of redesigning the rotor of the scaled model, so that a representative thrust of the full scaled aerodynamic force is obtained in the new rotor at the low Reynolds regime [1].

3. Description of the Ducted Fan/Software-in-the-Loop Method

A new approach to include a realistic scaled thrust dynamic force during the wave tank test has been implemented. The basic concept of this method consists of substituting the rotor by a fan driven by an electric motor. The fan thrust is controlled by the fan rotational speed set by the controller, which again depends on the real time simulation of the full scale rotor in a turbulent wind field, with the platform motions measured in real time in the wave tank test. The FAST code developed by NREL [5] was used for the simulation of the rotor thrust. This code has been extensively validated within the IEA Annex 30 (OC3) for the simulation of floating wind turbine including comparisons of the rotor aerodynamic thrust with other software [6]. We refer to the described method as Software-in-the-Loop (SIL).

3.1. Control of the Ducted Fan

The fan system used in the tests is composed of a brushless motor integrated with the ducted fan. The motor power electronics is regulated by an Electronic Speed Controller (ESC) card

that is powered by an industrial AC/DC power supply. The rpm of the motor is controlled by a Pulse Width Modulation (PWM) signal that is generated with the LabVIEW control software, using servo libraries for Arduino. The demanded force for the fan is provided by the full scale simulation of the rotor's aerodynamic thrust. The PWM signal has a variable period with a range between 1000ms (fan stopped) and 2000ms (fan at maximum power). The ESC model is a Jeti Spin 99 and can be configured and fine-tuned by a programming card that allows setting parameters as the timing of the motor, the type of power supply or the PWM-frequency. Figure 1 shows the layout of the system hardware. The selection of the power of the fan system is

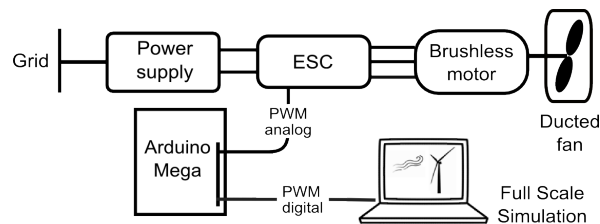


Figure 1. Fan Control System Lay Out

based on the range of required thrust during the test. This depends on the nominal power of the wind turbine and the scale factor. In addition, the thermal stability of the fan system has to be considered, in order to run at the required power during the requested time of the test and avoid using a cooling down phase.

3.2. Implementation of the Software-in-the-Loop System

The layout of the system is shown in Figure 2. The left side describes the simulation part of the system, which works in full scale, and the right side represents the wave tank scaled test. The different magnitudes that are interchanged between both blocks are transformed by the appropriated scaling laws based on the factor scale λ . The simulation tool provides the total aerodynamic force on the shaft F_{aero} from integration of all the aerodynamic loading at the blade elements. This force in full scale is transformed to the model scale (f_{aero}) and the pulse width of the PWM signal needed to produce the force in the ducted fan is provided by a calibration curve (see Section 4.3). The control system regulates the fan speed that introduces the desired force at the model's hub height. The waves produced by the wave maker are also acting over the platform and, together with the aerodynamic thrust, inducing motions. The acquisition system measures the positions and velocities for the 6 degrees of freedom of the platform at a certain sampling period. These measurements are sent to the simulation tool that is waiting for the data to advance one time step and calculate the new value of the aerodynamic thrust. For this reason, the sampling period, Δt , and the simulation time step, ΔT , have to be set accordingly (with a factor of $\lambda^{0.5}$).

This approach can obtain a realistic aerodynamic thrust on the scaled model. As the computation of the force takes into consideration the motion of the platform, the effect of the aerodynamic damping is included. In addition, the control actions, the different types of wind (turbulent, constant, gusts) and the operating condition (idling, power production, etc.) are taken into account for the calculation of the thrust at every instant of the test. The simplicity of the method makes it cost effective and flexible because the material is not specific for a certain wind turbine model and it could be used in different tests for different models. The main

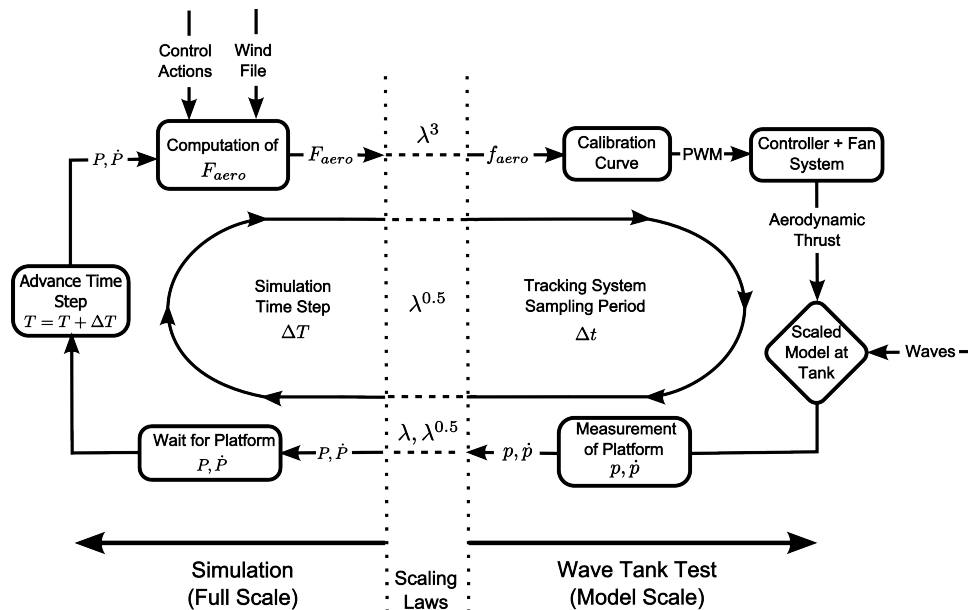


Figure 2. Software-in-the-Loop Method Diagram

drawback is that it does not match correctly the gyroscopic momentum or the aerodynamic torque. These effects are considered less important with respect to the global dynamics of floating wind turbines.

3.3. Communication Protocol

We have used the LabVIEW software to acquire the data from the wave tank motion capture system at ECN (Qualisys) and to communicate with the wind turbine simulation software during the test execution. A TCP/IP network protocol was selected for the communication between LabVIEW and Qualisys and also between LabVIEW and the simulation code.

4. Application to a Floating Wind turbine Scaled Test

The described methodology was applied during a test campaign of a floating semisubmersible platform performed during 2013 at the École Centrale de Nantes (ECN) wave tank in France. ECN's motion tracking system is very advanced and consists on 18 ProReflex cameras with a sampling frequency up to 120Hz and a precision of 1.2mm at a distance of 35m. The purpose of the test campaign was the verification of the platform design and also the assessment of the performance of the Software-in-the-Loop system.

4.1. Description of the Floating Wind Turbine Model

The platform concept that was tested at ECN is called "Concrete Star Wind Floater" and has been designed by Dr.techn.Olav Olsen AS (OO). It is an innovative semisubmersible design in concrete for a 6MW wind turbine. A sketch of the platform is provided in Figure 3. The data of the platform have been provided by OO. For the the wind turbine model, we have scaled the NREL Baseline 5MW wind turbine [7] to be representative of a 6MW wind turbine, according to the public available data of the Siemens SWT-6.0-120 turbine. First, we adjusted the original rotor diameter from 126m to 120m, keeping the same relative radial distribution

of chord, twist and airfoils. Then, we increased the rotor speed to obtain the Siemens 6MW nominal tip speed and we also increased the generator torque to match the nominal power. The main characteristics of the floating wind turbine are summarized in Table 1.

Table 1. General Parameters of the Floating Wind Turbine in Full Scale

<i>Property</i>	<i>Value</i>	<i>Comments</i>
Total Weight	10091.5t	Including turbine, solid/water ballast, outfitting etc.
RNA Mass	310t	-
Platform Mass	9431.5t	-
Center of Gravity	9.658m	Above keel. Full system.
Center of Buoyancy	7.046m	Above keel
Pitch/Roll Inertia	7.46E6t m^2	Referenced to platform center & waterline. Full system.
Yaw Inertia	4.5E6t m^2	Referenced to platform center & waterline. Full system.
Platform Draft	20m	-
Rated Wind Speed	12.7m/s	-

The mooring system is composed by three lines. The fairleads are located at the external cylinders surface, 14m below the Still Water Line (SWL). The anchors are located at a depth of 200m. The main parameters of the mooring system in full scale are shown in Table 2. The length of the two downwind lines (lines 2 and 3) has been reduced due to restrictions imposed by the dimensions of the wave tank (50m length, 30m width and 5m depth).

Table 2. Mooring System Parameters in Full Scale

	<i>Line 1</i>	<i>Line 2</i>	<i>Line 3</i>
Anchors radial position	829.23m	580.0m	580.0m
Fairleads radial position	32.5m	32.5m	32.5m
Angular position of anchors	180°	60°	300°
Angular position of fairleads	180°	60°	300°
Length	835.5m	586.27m	586.27m
Equivalent line diameter	0.126m	0.126m	0.126m
Mass density	106.77kg/m	106.77kg/m	106.77kg/m
Axial stiffness	7.536E8N	7.536E8N	7.536E8N

4.2. Scaled Model

Froude scaling was applied to the model building using a scale factor of 1/40. The structural stiffness was not scaled, instead, the model can be considered rigid. A complete description of the scaled model is provided in [8]. As has been described in Section 3, a ducted fan substitutes the whole rotor in the scaled model. For the full scaled rotor of our 6MW wind turbine, we estimated an expected maximum peak of aerodynamic thrust of around 1500kN. Therefore, we chose a fan with a maximum thrust of 3kg (around 1900kN in full scale) that could reproduce

the expected force with a comfort margin. The mass of the fan is around 0.5kg which is not enough to represent the 310t that weights the RNA in full scale. Therefore, we included some ballast at the scaled model tower top to match the required weight. Figure 4 shows an image of the scaled model in the basin with the ducted fan on top during a test.



Figure 3. Concrete Star Wind Floater

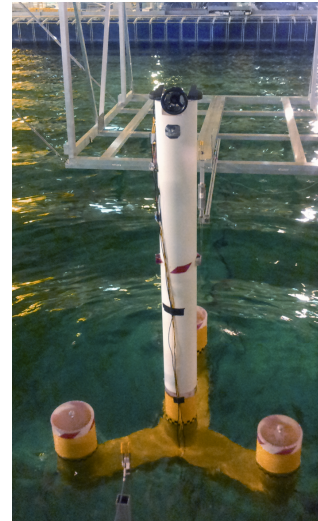


Figure 4. Scaled Model in the Wave Tank

4.3. Calibration of the Ducted Fan

The relationship between the PWM signal and ducted fan thrust was obtained by a static calibration. Figure 5 shows the installation of the fan on a cantilevered horizontal steel plate equipped with strain gages. With the fan disconnected, we loaded the plate with a set of weights to obtain a relation between the different weights and the plate deformation. Afterwards, we unloaded the plate, and connected the fan at different powers, measuring the deformation against the pulse width. We established the relationship between the PWM period and the static force of the fan with an error below 0.8% at medium and high power and below 2.5% at low power.



Figure 5. Fan Set Up for Calibration

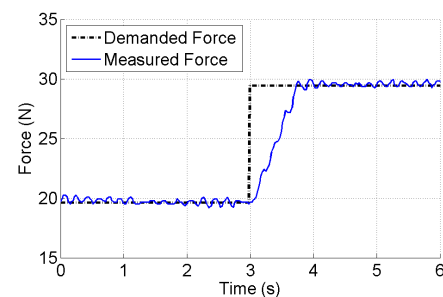


Figure 6. Fan Response to Step Demand

4.4. Dynamic Response of the Fan

We assessed the capability of the fan system to react to the required changes in thrust by demanding the fan a step change in the force and evaluating the delay in the response. Figure 6 shows the response of the fan to a step change in the demanded force of 9.8N (1kg). The noise in the measured force is due to vibrations in the beam/strain gauge setup excited by the fan. The slope of the measured force is 13.43N/s (136 kN/s in full scale). We performed a combined wind and wave simulation of our full scale wind turbine model, using a turbulent wind of 12.7m/s mean wind speed and 19% of turbulence intensity and waves with $H_s=2.6\text{m}$ and $T_p=7.3\text{s}$. From the thrust signal (Figure 7) we estimated that the maximum rate of change of the thrust is approximately 140kN/s (Figure 8). The ducted fan therefore seems to have adequate response in terms of thrust force rate of change, but this is clearly just the first of several required tests, where the next ones will include phase information.

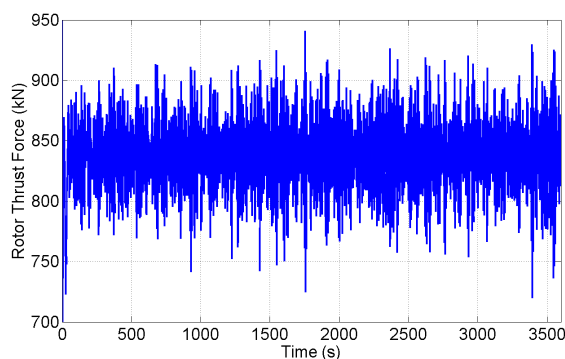


Figure 7. Computed Thrust Force

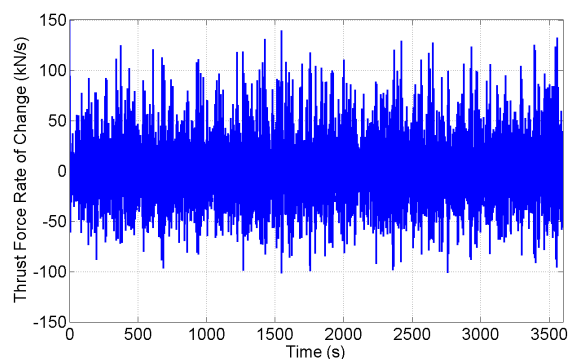


Figure 8. Thrust Force Rate of Change

5. Discussion of the Results

The results of the experiments are discussed in the next sections in comparison with FAST full scale computations. The results are presented in full scale.

5.1. Static Wind Tests

A set of tests in still water with different constant wind speed loadings were performed to verify the static performance of the fan system. In addition to the rated wind speed (12.7m/s) two lower wind speeds (5m/s and 8,5m/s) were chosen and also a higher wind speed of 25m/s.

The results show a good agreement between measurements and computations for the surge and pitch displacements with the exception of the surge displacement for the wind speed of 12.7m/s. The computed displacement at this wind speed is 14% higher than the experimental. The surge displacement seems to be sensitive to small changes on the mooring parameters, in particular at rated wind speed. Some uncertainty on the value of some parameters of the mooring system exists that could cause the differences in surge at 12.7m/s. The agreement on the pitch angle between tests and simulations shows that the fan introduced the correct static force.

5.2. Free Decay Tests

Based on the free decay tests on surge, heave and pitch of the moored platform we adjusted the damping level of the system in our computational model. Quadratic damping was added to take the viscosity into account.

For the pitch degree of freedom, in addition to a regular test, we performed a second free decay

including the aerodynamic loading of a constant wind of 12.7m/s. This second test allowed assessing the effect of the aerodynamic loading on the pitch behavior of the platform. The wind speed of 12.7m/s produces the maximum thrust on the rotor and it is just in the transition between the wind turbine control regions 2 and 3. Therefore, pitch control is activated in this case. Figure 9 presents a comparison of both platform pitch free decay tests, with and without wind, with computations.

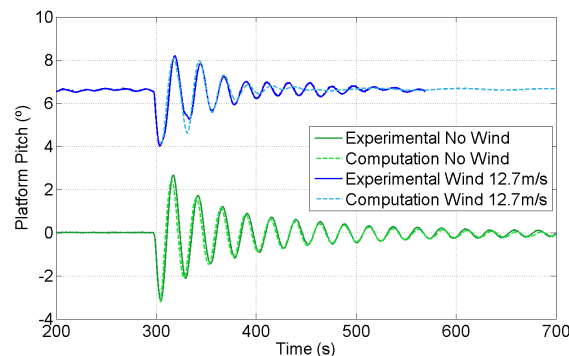


Figure 9. Experimental and Computed Pitch Free Decay with & without Wind Loading

In the free decay tests with no wind loading, the platform oscillates around the 0° position. The correspondence between measured data and computation is good. The same free decay tests performed with a constant wind of 12.7m/s are represented. In this case, the loading at the rotor produces a pitch on the platform that oscillates around 6.5° . The match between the experimental results and the computation in the free decay case including wind is fairly good. The experiment shows a very good agreement on the damping of the highest oscillations. The difference seen in the second valley is probably due to imperfect pitch excitation in the experiment. The damping ratio of the case with wind loading (0.033) is lower than in the case with no wind (0.086) due to the effect of the pitch control that is simulated by the SIL. A low amplitude oscillation persists in the tests data that is not present in the simulation case. This effect is due to excessive filtering of the motion signal that fed the SIL system during the test, not allowing the fan to respond to low amplitude oscillations. This issue will be improved in future campaigns.

5.3. Combined Irregular Waves and Turbulent Wind Tests

Two different environmental conditions were defined to test the behavior of the platform under combined irregular waves and turbulent wind. The first sea state had a significant wave height, H_s , of 1.96m and a peak period, T_p , of 6.5s and was combined with a turbulent wind of 8.5m/s mean speed and 23% turbulence intensity. The second state corresponded to a sea with $H_s=2.64$ m, $T_p=7.3$ s and a mean wind speed of 12.7m/s with 19% turbulence intensity. A JONSWAP spectrum was used for the generation of the irregular waves and the winds followed a Kaimal turbulence model. The wave spectrums used in the simulations were obtained by analysis of the measured wave height time series in the experiment. The resulting γ shape factor for the first sea state is estimated to be 2.87 and 5.0 for the test cases excluding wind and including wind, respectively, and 4.0 for both test cases of the second sea state. The Figures 10 and 11 show the surge and pitch response for the first sea state with and without the turbulent wind of 8.5m/s. Data from both tests and computations have been included. Figures 12 and 13 plot the same data for the second environmental state. The duration of the time series to

obtain the PSD's was 3800s. The absolute values of the surge and pitch PSD's are not shown for confidentiality reasons. Instead, PSD's have been normalized using as factor the value of the respective PSD (surge or pitch) at T_p for the second sea state experimental data including wind, where the motion is larger.

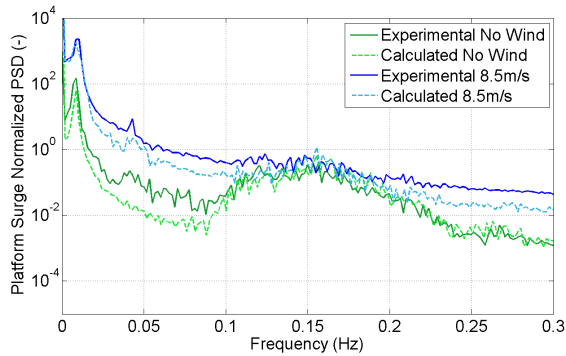


Figure 10. Surge PSD $H_s=1.96m$ $T_p=6.5s$

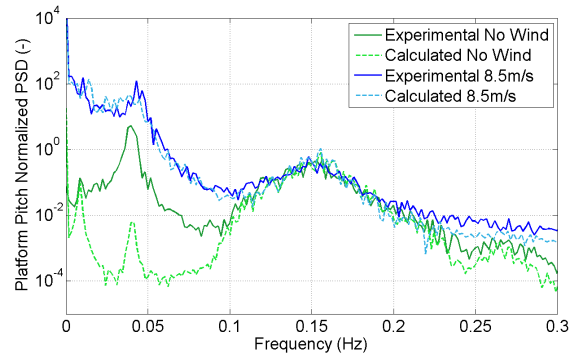


Figure 11. Pitch PSD $H_s=1.96m$ $T_p=6.5s$

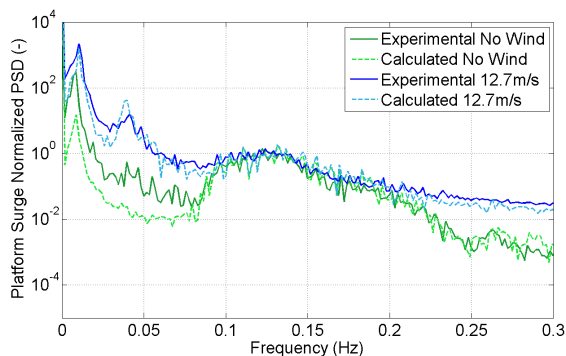


Figure 12. Surge PSD $H_s=2.64m$ $T_p=7.3s$

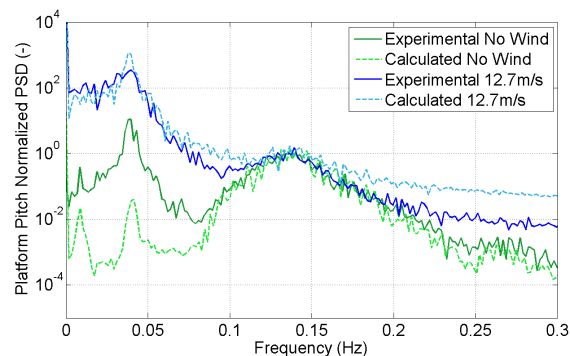


Figure 13. Pitch PSD $H_s=2.64m$ $T_p=7.3s$

Important differences in the magnitude of the motion appear between cases with wind and those excluding it. As the wind has low frequency variations, these differences are more pronounced between 0 and 0.1Hz. They are also more important for the pitch degree of freedom than for the surge. The concordance between tests and simulations for the cases with wind is very good in both environmental conditions and both for surge and pitch, showing the correct performance of the ducted fan and SIL method. Around T_p , where direct wave loading is more important, the surge and pitch motions are similar in all the series. The wind turbulence excites additional motions away from T_p , both at higher and lower frequencies, because the turbulence is more important relative to the low wave excitation. Some important disagreements at low frequencies in pitch, but also in surge, appear in the wave only cases between tests and simulations when the aerodynamic loading is not driving the platform motions. As will be discussed later, the reason for this discrepancy could be a difference in the wave energy at low frequencies between the wave tank and our computations and also second order effects that are not captured by FAST.

For the surge displacement in both sea states (Figures 10 and 12), two main peaks appear in the PSD's. The first one corresponds to the surge natural frequency (0.011Hz) and the second one is located around T_p of the wave spectrum. The agreement in the peak amplitude between test

and simulation is very good both in cases with and without wind. A certain discrepancy exists on the surge energy at low frequency (around 0.05Hz), specially for the 8,5m/s wind speed case. For the pitch PSD's (Figures 11 and 13) two main peaks also arise: one at the pitch natural frequency (0.043Hz) and another around T_p of the wave spectrum. The amplitude of the PSD for all the series matches very well in the proximity of T_p , where more direct wave loading exist, but around the natural frequency the amplitude for the no wind case is much lower in the computation than in the results obtained in the wave tank. This is the main discrepancy found between experiments and computations. When the wind loading is introduced, the magnitude of the peak matches very well between tests and simulation, because the wind loading influences the pitch motion more than waves.

Figure 14 compares the PSD of the wave height for the experimental and computational time series to illustrate the differences in the wave energy between the wave tank and our computations. The wave generated in the tank presents more energy at low frequencies than the computation, and this could excite more the pitch natural frequency and also the surge, explaining in part the mentioned discrepancies in the motions between the no wind tested and computed cases. Second order slow-drift hydrodynamic effects are not captured by the simulation software that we have used and this can also contribute to the differences.

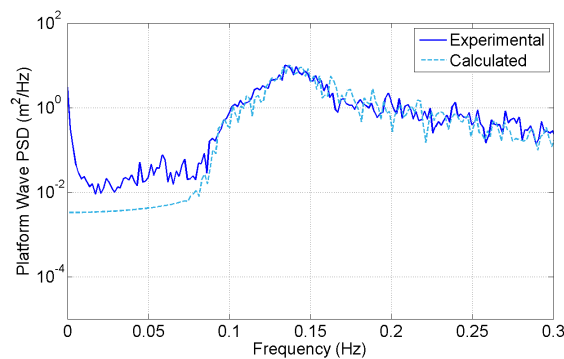


Figure 14. Experimental and Computed Wave Spectrum $H_s=2.64\text{m}$ $T_p=7.3\text{s}$

6. Conclusions

A new methodology for the scaling of aerodynamic loading during combined wave and wind scaled tests at wave tank has been presented. The method uses a ducted fan governed by a real time computation of the full rotor coupled with the platform motions during the test.

The methodology has been applied to the test of a 6MW semisubmersible floating wind turbine in the ECN wave tank. The experimental results have been compared with computations, in general with good correspondence. Static tests and free decay tests have been useful to verify settings of our computational model: mass and inertia distribution, damping, mooring line stiffness, etc. In addition, the platform pitch displacements under different constant wind loading compare well between tests and computations, showing the correct static performance of the ducted fan system. The free decay test in pitch under a constant wind of 12.7m/s illustrates the capability of the fan to capture the coupling of the aerodynamic thrust with the rotor's relative displacements within the wind field. Finally, the PSD's of the platform surge and pitch motions under irregular waves, without wind loading, present a certain disagreement, due to differences on the wave spectrum and second order hydrodynamics. Nevertheless, when the turbulent wind is included to the irregular wave cases, these differences disappear, and the

experimental results match very well the computations. In particular the effect of wind over the pitch motion is very accurately captured, which is important to calculate the correct rotor loads.

The performance of the ducted fan and SIL system has been successfully validated though we plan to further validate it in future campaigns. The methodology is very promising, furthermore, considering the low cost of the system and its versatility to be used in different test campaigns.

7. Acknowledgments

We want to acknowledge Carlos López Pavón and Daniel Merino Hoyos: this method was applied for the first time with them in collaboration between Acciona Energía and CENER within the EOLIA project. We also want to give thanks to Trond Landbø, from OO, Hugo Ramos and Leo González from Universidad Politécnica de Madrid, and Jean Marc Rousset, Sylvain Bourdier and Laurent Davoust from ECN.

We are very grateful to the MARINET program that granted our group with free of charge access to the ECN facilities. Part of this work has been funded by the INNWIND.EU and NOWITECH projects.

References

- [1] Matthew J F, Kimball W K, Thomas D A and Goupee A J *Design and Testing of Scale Model Wind Turbines for Use in Wind/Wave Basin Model Tests of Floating Offshore Wind Turbines*, Proc 32nd ASME International Conference on Offshore Mechanics and Arctic Engineering, Nantes, France, 2013.
- [2] Bredmose H, Larsen S E, Matha D, Rettenmeier A, Marino E and Sætran L *Collation of offshore wind-wave dynamics*, MARINET, 2012.
- [3] Roddier D, Cermelli C, Aubault A and Weinstein A *WindFloat: A Floating Foundation for Offshore Wind Turbines*, Journal of Renewable and Sustainable Energy 2 033104, 2010.
- [4] Robertson A N, Jonkman J M, Goupee A J, Coulling A J, Prowell I, Browning J, Masciola M D and Molta P *Summary of Conclusions and Recommendations Drawn from the DeepCwind Scaled Floating Offshore Wind System Test Campaign*, Proc 32nd ASME International Conference on Offshore Mechanics and Arctic Engineering, Nantes, France, 2013.
- [5] Jonkman J M *Dynamics Modeling and Loads Analysis of an Offshore Floating Wind Turbine*, Technical Report NREL/TP-500-41958, 2007
- [6] Jonkman J, Larsen T, Hansen A, Nygaard T, Maus K, Karimirad M, Gao Z, Moan T, Fylling I, Nichols J, Kohlmeier M, Pascual J and Merino D *Offshore Code Comparison Collaboration within IEA Wind Task 23: Phase IV Results Regarding Floating Wind Turbine Modeling*, European Wind Energy Conference (EWEC), Warsaw, Poland, 2010.
- [7] Jonkman J M, Butterfield S, Musial W and Scott G *Definition of a 5-MW Reference Wind Turbine for Offshore System Development*, Technical Report NREL/TP-500-38060, 2009
- [8] Kelberlau F, Lawrenz M and Nygaard T A *Free Decay Testing of a Semisubmersible Offshore Floating Platform for Wind Turbines in Model Scale*, MSc Thesis, UNI Kassel and the Norwegian University of Life Sciences, 2013.